PERGAMON

Journal of Geodynamics 33 (2002) 53–63

JOURNAL OF
GEODYNAMICS

www.elsevier.com/locate/jgeodyn

GOCE closed-loop simulation

H. Oberndorfer*, J. Müller

Institute for Astronomical and Physical Geodesy, Technische Universität München, 80290 Munich, Germany

Abstract

GOCE (gravity field and steady-state ocean circulation explorer) will provide a global model of the Earth's gravity field with high spatial resolution and high accuracy. The gravity measurements are derived from a combination of different sensor readouts. On one hand, the satellite itself is the test mass which is tracked by GPS, on the other hand, accelerometers are combined to a gradiometer to measure gravity gradients. To extract the gravitational signal, it is necessary to observe the non-gravitational forces disturbing the satellite dynamics, and to control these effects by thrusters or correct them in post-processing. Therefore GPS, star trackers and the gradiometer are employed for orbit control, attitude control, precise positioning and gravity field measurements. This paper focuses on the investigation of the accuracy of gradiometer measurements which depend on the complete system performance. The gradiometer measurements were simulated as time series using the software SIMULINK. Differences between input gravity gradients and simulated gradiometer measurements served as input for the derivation of error power spectral densities (PSD's). The latter are used for further error analyses of the scientific end-products (e.g. spherical harmonic coefficients, geoid heights, gravity anomalies). The errors to be considered are caused by the imperfection of any sensor or actuator and their measurement noise. Moreover, the geometry (position and orientation) of the several instruments with respect to each other have been taken into account with a certain accuracy. All these errors and their couplings affect the measurements and consequently the end-products. In terms of power spectral densities, the mission requirement of the gradiometer is 4 mE/$\sqrt{\text{Hz}}$ white noise with a $1/f$-behaviour below 1 mHz. Analyses and simulations allowed the determination of the full error budget in the spectral domain, based on all types of realistic error sources. The main error sources have been identified and it could be shown that the mission requirements are fulfilled.

* Corresponding author. Tel.: +49-89-289 23185; fax: +49-89-289-23178.
E-mail addresses: helmut@alpha.fesg.tu-muenchen.de (H. Oberndorfer), resp.jxmx@bv.tum.de (J. Müller).

0264-3707/02/$ - see front matter © 2002 Published by Elsevier Science Ltd.
PII: S0264-3707(01)00054-0

1. Introduction

The launch of the GOCE mission is envisaged for the year 2004. This project is the first selected mission of ESA's earth explorer programme (GOCE Phase B will start in November 2000). A combination of different sensors is used to measure the spatial variations of the gravity field on board an Earth orbiting spacecraft with high accuracy. The satellite itself is a test mass whose orbit is tracked by GPS (high-low satellite-to-satellite tracking, SST). The main measurement instrument for the gravity gradients is the gradiometer (satellite gravity gradiometer, SGG), a combination of several accelerometers. The observations are acceleration differences over a short baseline which represent the linear approximation of the second derivation of the gravity potential, the gravity gradients. ESA's requirement for the accuracy of the measured diagonal elements of the gravity gradient tensor in the frequency band between 0.005 and 1 Hz is 4 mE/$\sqrt{\text{Hz}}$ (1 E = 1 eötvös = $10^{-9}/\text{s}^2$) or better.

The gradiometer measurement accuracy can be simulated in two ways. The first one is by the calculation of the error PSD's of the gravity gradients in the frequency domain. Here, the input time series are transformed into power spectral densities by using the FFT transformation, whereas the error PSD's of the gravity gradients are computed by multiplying the signals with corresponding transfer functions. This method works only when the models depend on linear differential equations. Otherwise one has to compute convolutions of the signals in the frequency domain. The second method is based on the simulation of the measurements in the time domain, where it is easy to multiply signals, using adequate models. Here, the models incorporated can be more complicated. We used both methods. First we designed a gradiometer simulator based on the dynamic accelerometer model provided by ONERA (Willemenot, 1998). Then we modeled the complete satellite system including star sensor, GPS, control systems, thrusters and satellite dynamic model and combined all models to a complete system model.

The goal of the gradiometer simulation is to check if the requirements for the mission are fulfilled and to identify the main error sources.

2. GOCE system model

In the flow chart (Fig. 1) the interaction between forces, sensors and control loops is shown. It is the basis for the closed-loop simulation. The central block represents the satellite platform with the gradiometer instrument mounted on it. All linear forces acting on the platform/accelerometer frame, are focused on the center of mass. Forces are listed in the first line, torques on the right upper block, angular effects in the third line. The left block shows the orbit maintenance and the control of the linear accelerations, the right block indicates the attitude control. The linear acceleration control is divided into orbit maintenance and drag control in an extended measurement bandwidth (MBW). The input for attitude and drag-free control is obtained from the high-low SST measurement with GPS and gradiometer observations. The angular control is shown in the right block where the combination of star tracker and gradiometer measurements is used to estimate angular velocities and to control the angular accelerations of the satellite. The main instrument is the gradiometer, consisting of six accelerometers. In the flow chart only two of them are shown. On each axis of an assumed coordinate triad two accelerometers are mounted, one on the positive, the other on the negative side (see Fig. 2).

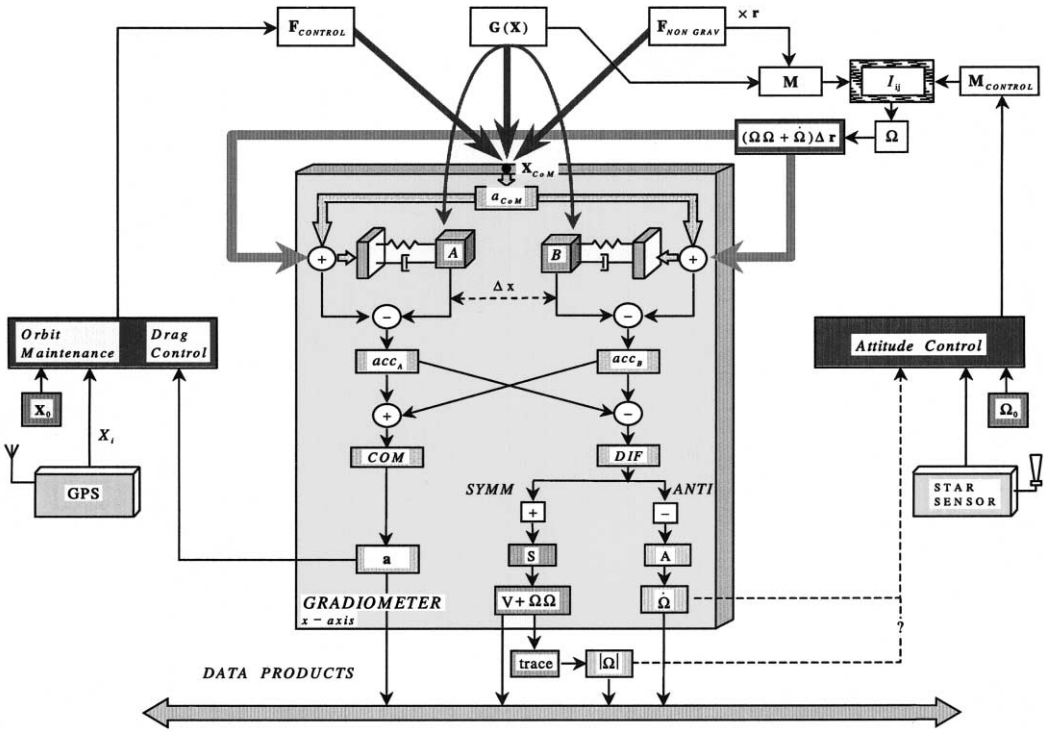

Fig. 1. Closed-loop interaction of satellite, sensors and sub-systems.

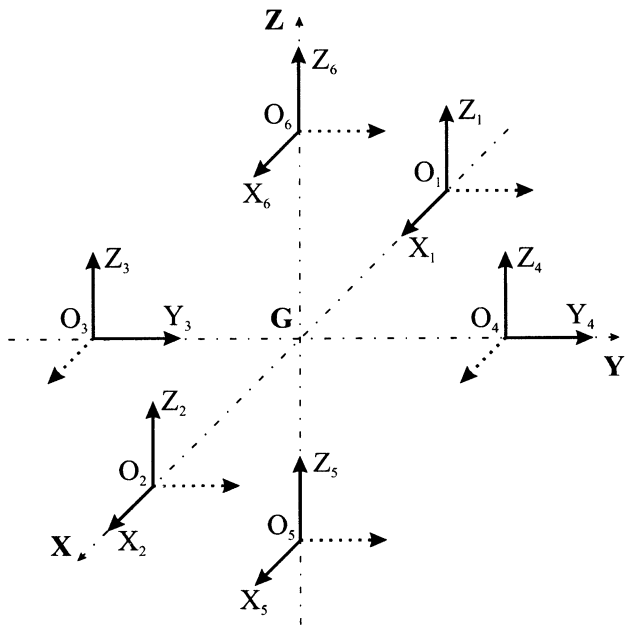

Fig. 2. Non-symmetric diamond gradiometer configuration.

From the read-out of two accelerometers in the same direction, both the difference and the mean are derived. The former is denoted differential mode, the latter common mode acceleration. This procedure is shown in the flow chart (Fig. 1) below the two accelerometers A and B. The common mode acceleration contains all effects that lead to a linear disturbance of the satellite motion like drag forces, imperfections in the thrusters, and so on. Together with GPS observations, the common mode acceleration is used for orbit restitution and drag-free control (DFC). On the other hand, the GPS measurement and the common mode acceleration are the basis for high-low SST. The differential mode signal, divided by the baseline length, yields the gradiometer signal, one single component of Γ_{ik} the measurement tensor. Since the observations are performed on a rotating platform, inertial forces (centrifugal and Euler) are sensed as given by

$$\Gamma_{ik} = V_{ik} + \Omega_{ij}\Omega_{jk} + \dot{\Omega}_{ik}. \tag{1}$$

The gradiometer measurement tensor Γ_{jk} depends mainly on angular accelerations $\dot{\Omega}_{ik}$ and the square of the angular velocities $\Omega_{ij}\Omega_{jk}$ of the satellite. These tensors read

$$\dot{\Omega}_{ik} = \begin{pmatrix} 0 & \dot{\Omega}_z & -\Omega_y \\ & 0 & \dot{\Omega}_x \\ \text{anti-symm.} & & 0 \end{pmatrix}, \tag{2}$$

$$\Omega_{ij}\Omega_{jk} = \begin{pmatrix} -\Omega_y^2 - \Omega_z^2 & \Omega_x\Omega_y & \Omega_x\Omega_z \\ & -\Omega_x^2 - \Omega_z^2 & \Omega_y\Omega_z \\ \text{symm.} & & -\Omega_x^2 - \Omega_y^2 \end{pmatrix} \tag{3}$$

The coordinate directions pertain to a local co-rotating triad with along-track (x), cross-track (y) and radial direction (z) axis. Γ_{ik} serves as input for the further processing of gravitational products and rotational quantities. Ideally, the tensor Γ_{ik} can be split in a symmetric and an anti-symmetric part, which can be used to separate the gravitational and the rotational contributions. The anti-symmetric part of the tensor represents the angular accelerations. The symmetric part of the tensor represents the sum of the gravity signal and the angular velocities. Subsequently, the angular acceleration $\dot{\Omega}_{ik}$ are used as input for the attitude control system (ACS). The ACS is further aided by star sensors. As a consequence of the Earth pointing attitude only the angular velocity Ω_y is large and has to be corrected, the other angular velocities are controlled by the ACS so that their residual influence can be considered as noise.

Simulations have shown that the signal of Ω_x^2, $\Omega_x\Omega_z$, and Ω_z^2 in the MBW are less than 1e-4 E/$\sqrt{\text{Hz}}$. The signal of Ω_y^2 is the square of the orbit frequency which is of the order of 1 E/$\sqrt{\text{Hz}}$. There are two possible methods for the calculation of the angular velocity about the cross track axis, Ω_y,

- to integrate the angular accelerations $\dot{\Omega}_{ik}$ or
- to use the tracelessness property of the measurement tensor.

When applying the first method, a complementary filtering of the angular accelerations together with the attitude angles measured by the star sensor is necessary. Moreover, a special gradiometer

configuration, as indicated in Fig. 2, has to be chosen. By correcting the measurement tensor with the estimated Ω_y^2 term, the pure gravity gradient tensor V_{ik} is obtained.

3. Gradiometer configuration

For the GOCE gradiometer, six accelerometers were arranged in a so called non-symmetric diamond configuration. This became necessary, because not all axes of the ONERA accelerometers achieve the same precision, the accelerometers have only two sensitive axes, the third one is less sensitive by a factor of 1000. In Fig. 2 the selected gradiometer configuration is shown, where the dots indicate the less sensitive axis. As a consequence, not all tensor components can be observed. To obtain the angular velocity about the cross track axis, Ω_y, with high accuracy, it is necessary to measure the Γ_{xz} and Γ_{zx} components with the high sensitive accelerometer axes. The best gradiometer configuration for this purpose is the non-symmetric diamond configuration (Fig. 2). This gradiometer has the feature to measure the diagonal components Γ_{ii} directly with high accuracy as well as the two off-diagonals which are needed to determine Ω_y^2 from the integrated anti-symmetric measurement tensor. But the accuracy of the less sensitive components, V_{xy} and V_{zy}, is then restricted to about 1 E/$\sqrt{\text{Hz}}$ only.

4. Instrument noise

The GOCE accelerometers are developed by ONERA (Willemenot, 1998; Willemenot and Touboul, 1998). The basic working principle of these instruments is electrostatic suspension of a test mass in the center of a cage, which is controlled by a capacitive position detector.

The GOCE accelerometers (see Fig. 3) can be described by three blocks and one feedback loop, the test mass dynamics block for the interactions between the test mass and the electrodes, the position detector and the PID-controller. In reality, the situation is more difficult, but the main dynamics of the accelerometer is described very well by this simple scheme. The single blocks can

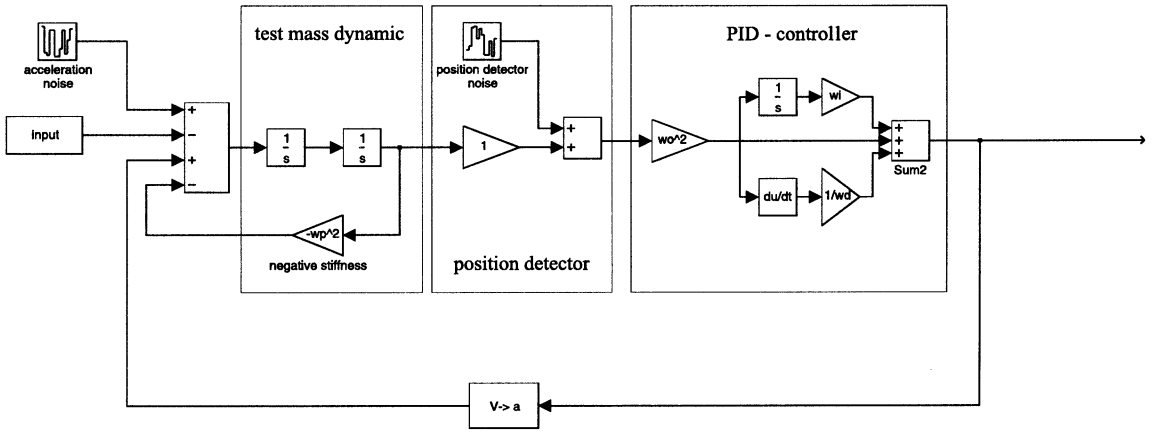

Fig. 3. Simulation model and elements of the accelerometer.

be modeled by transfer functions. The test mass dynamics describes the sensitivity of the test mass to input and control accelerations where the limiting factor is the negative stiffness of the loop: the lower the stiffness the higher the sensitivity of the instrument. The position of the test mass is measured by the position detector which is driven by a carrier frequency of 100 kHz. The position sensor is simulated with a transfer function of one, but with additional noise. The output of the position detector is used to drive the feedback voltage by the PID-controller. The PID-controller is operating in a bandwidth from DC to 150 Hz which limits the calculation of the derivative of the signal. As a result of the feedback, the position sensor noise, amplified by the controller, couples with the test mass dynamics and produces a large noise level which increases proportional to f^2. The accelerometer transfer function models the reaction of the accelerometer to input accelerations. In the ideal case, it should be one which is approximately true at frequencies much lower than the resonance frequency of the accelerometer. At higher frequencies the transfer function of the accelerometer decreases. All internal effects and error sources within one accelerometer are summarized by two kinds of noise, the acceleration noise and the position sensor noise. A more detailed list of these internal error sources and their power spectral densities was provided by ONERA. It includes noise, fluctuation of the bias, thermal sensitivity of the bias and others. In detail, there have been considered:

- radiometer effect,
- radiation pressure effect,
- Earth magnetic field,
- spacecraft magnetic effect,
- Lorentz force effect,
- cage dissymmetry,
- capacitive sensor bias,
- capacitive sensor noise,
- drive voltage amplifier noise,
- contact potential differences,
- residual gas damping,
- wire stiffness,
- wire damping,
- measurement pick-off.

We used the simple accelerometer noise model in our simulations, to avoid the implementation of all the individual effects indicated. This simplification, combining all errors into two kinds of noise sources, speeds up the simulation. The model contains still another simplification. The real accelerometer controls six degrees of freedom of the test mass, but we simulated just control loops for the linear motion of the test mass. The sample frequency of the scientific measurements and down-linked data of the gradiometer should be 1 Hz. However, when one samples the real accelerations or gradiometer measurements at 1 Hz one obtains big aliasing errors because of the high frequency noise. To avoid it, one has to use an anti-aliasing filter (i.e. a kind of a low-pass filter) before sampling. But the filter itself produces again an error. This error can be minimized by using a higher sampling frequency and by optimizing the filter. We used a sampling frequency of 10 Hz.

The accelerometer instrument noise calculated in the frequency domain is shown in Fig. 4 as error PSD. The structure of the PSD is a $1/f$ increase at low frequencies with a corner frequency of 10^{-2} Hz and a f^4 increase at frequencies higher than 0.1 Hz. The effect of the anti-aliasing filter is also indicated in Fig. 4, it reduces the high frequency noise after a maximum around 1 Hz. The error PSD of the less sensitive axis is by a factor 1000 worse than the other two. In Fig. 5, the simulated gradiometer instrument noise of the sensitive axes is plotted. It is in good agreement with the theoretical accelerometer noise, shown in Fig. 4, when we take into account a factor $\sqrt{2}$ which results from the combination of two accelerometer noises to the gradiometer noise.

5. Coupling errors

The physical mounting of the accelerometers, but also the physical mounting of the gradiometer in the satellite frame is not perfect. The approximation of the test mass dynamics and the non-ideal mounting affect the transformation between measured accelerations $\vec{\Gamma}_A$ and real accelerations $\vec{\lambda}_A$. This leads to a set of parameters describing the gradiometer measurement model.

The measurement equation of accelerometer A is:

$$\vec{\Gamma}_A = \vec{K}_{0A} + \vec{K}_{1A}\vec{\gamma}_A + \vec{K}_{lmA}\vec{\gamma}_A + \vec{K}_{2A}\vec{\gamma}_A\vec{\gamma}_A + \text{noise} \tag{4}$$

with

$\vec{K}_{0A}$ bias vector of accelerometer A,
$\vec{K}_{1A}$ scale factor diagonal matrix of accelerometer A,,

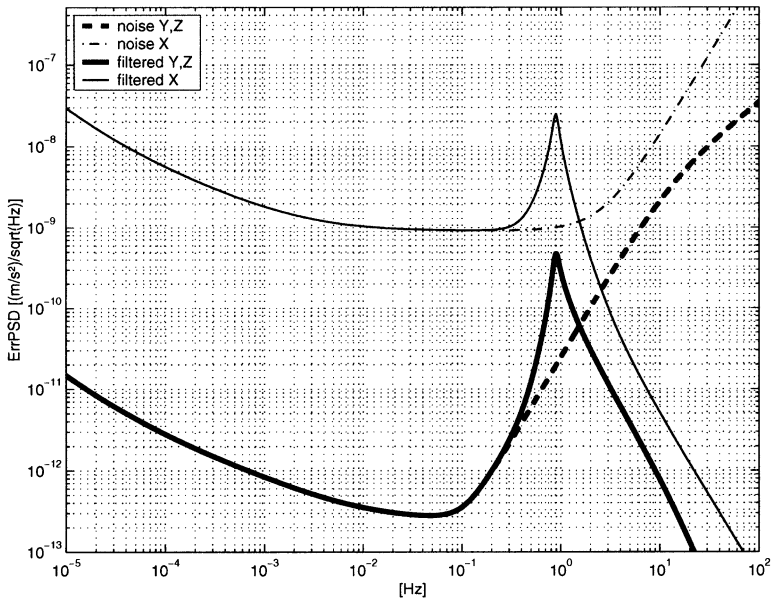

Fig. 4. Accelerometer instrument noise.

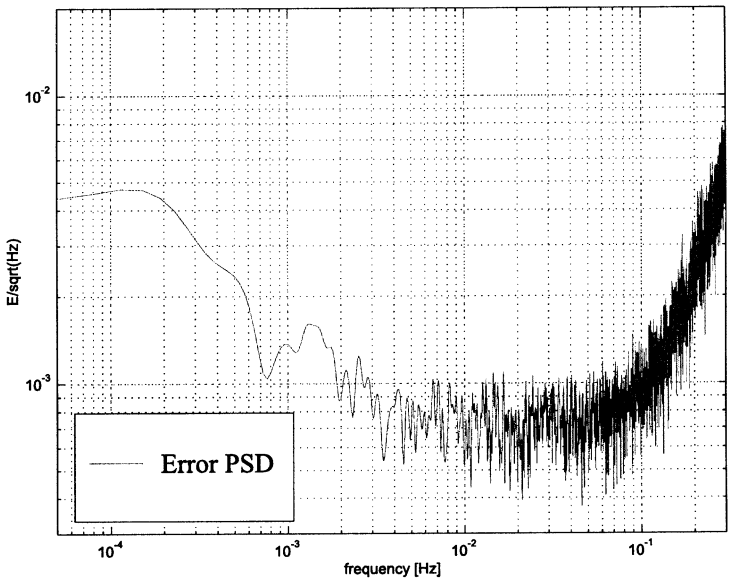

Fig. 5. Simulated accelerometer noise.

$\vec{K}_{2A}$ quadratic factor of accelerometer A,,
$\vec{K}_{lmA}$ misalignment and cross coupling matrix of accelerometer A.

The measurement equation of the gradiometer AB in the differential mode reads:

$$\vec{\Gamma}_A - \vec{\Gamma}_B = \left(\vec{K}_{0A} - \vec{K}_{0B}\right) + \left(\vec{K}_{1A}\vec{\gamma}_A - \vec{K}_{1B}\vec{\gamma}_B\right) + \left(\vec{K}_{lmA}\vec{\gamma}_A - \vec{K}_{lmB}\vec{\gamma}_B\right) + \left(\vec{K}_{2A}\vec{\gamma}_A\vec{\gamma}_A - \vec{K}_{2B}\vec{\gamma}_B\vec{\gamma}_B\right) + \sqrt{\text{noise}_A^2 - \text{noise}_B^2}. \quad (5)$$

It can be written with common and differential mode parameters:

$\vec{K}_{0dAB} = \vec{K}_{0A} - \vec{K}_{0B}$ bias vector of the gradiometer AB in differential mode,
$\vec{K}_{1\text{dAB}} = \vec{K}_{1A} - \vec{K}_{1B}$ differential scale factor diagonal matrix of the gradiometer AB,
$\vec{K}_{1cAB} = \vec{K}_{1A} + \vec{K}_{1B}$ common scale factor diagonal matrix of the gradiometer AB,
$\vec{K}_{2dAB} = \vec{K}_{2A} - \vec{K}_{2B}$ differential quadratic factor of the gradiometer AB,
$\vec{K}_{1cAB} = \vec{K}_{2A} + \vec{K}_{2B}$ common quadratic factor of the gradiometer AB,
$\vec{K}_{lmdAB} = \vec{K}_{lmA} - \vec{K}_{lmB}$ differential misalignment and cross coupling matrix of the gradiometer AB,
$\vec{K}_{lmcAB} = \vec{K}_{lmA} + \vec{K}_{lmB}$ common misalignment and cross coupling matrix of the gradiometer AB.

The scale factor diagonal matrix, the misalignment and cross coupling matrix can be summarized in a common matrix:

$\vec{K}_{dAD} = \vec{K}_{1A} - K_{lmA}$,
$\vec{K}_{cAD} = \vec{K}_{1A} + K_{lmA}$,

These terms cause that other signals (e.g. gravity, rotation, non-gravitational forces) couple in the measurement. The effect of coupling errors (without the quadratic errors) was simulated and the results are shown in Fig. 6. The coupling errors play only a minor role for GOCE if the basic assumptions are valid.

6. Satellite pointing errors

A second effect of coupling errors has been taken into consideration. The gradiometer is not aligned exactly with the orbit system, because the satellite pointing is not exact. As a consequence, the gradiometer measures a rotated gravity gradient tensor. But the knowledge of only five tensor elements with highest precision makes it impossible to rotate the tensor back. A strong requirement for the pointing accuracy is needed. It is about 1 mrad for each axis. The error of the coupling of the satellite pointing with the gravity gradients is shown for the independent tensor components in Fig. 7.

In the low frequency part, up to 1e-3 Hz, the pointing error is the largest error source. The simulation has further shown, that the error of G_{xx}, G_{xy} and G_{yy} is about 1e-4 E/$\sqrt{Hz}$ at 5e-3 Hz. The error of G_{xz} and G_{yz} is about a factor 1000 higher.

7. Complete error model and conclusion

The result of the complete closed-loop gradiometer simulation (i.e. all error effects are switched on) is shown in Fig. 8. The resulting error spectra are the root sum squares of single error effects.

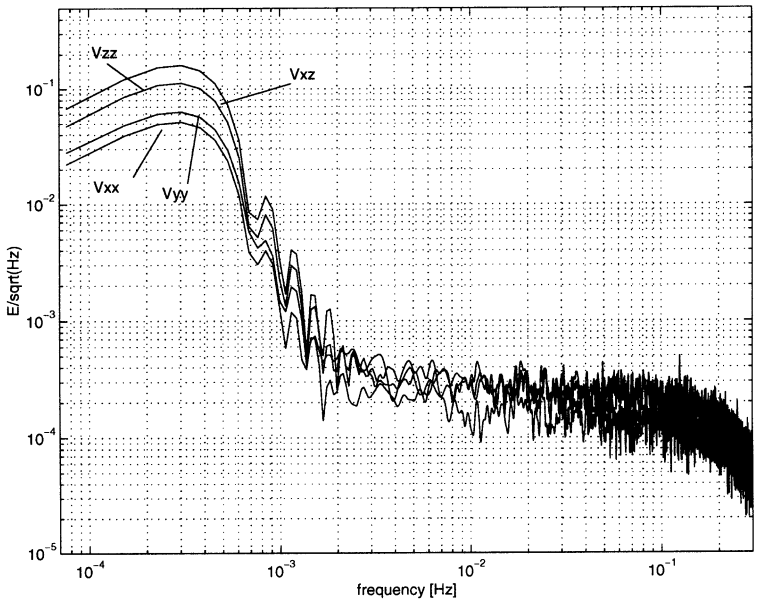

Fig. 6. Simulated coupling errors.

The results of the simulation in the time domain are comparable to the results in the frequency domain. The effect of the satellite pointing makes it impossible to measure the V_{xz} gravity gradient with the same accuracy as the diagonal components. But the non-symmetric diamond gradiometer configuration enables the estimation of Ω_y^2 (from Γ_{xz} and Δ_{zx} which is used to separate the measured

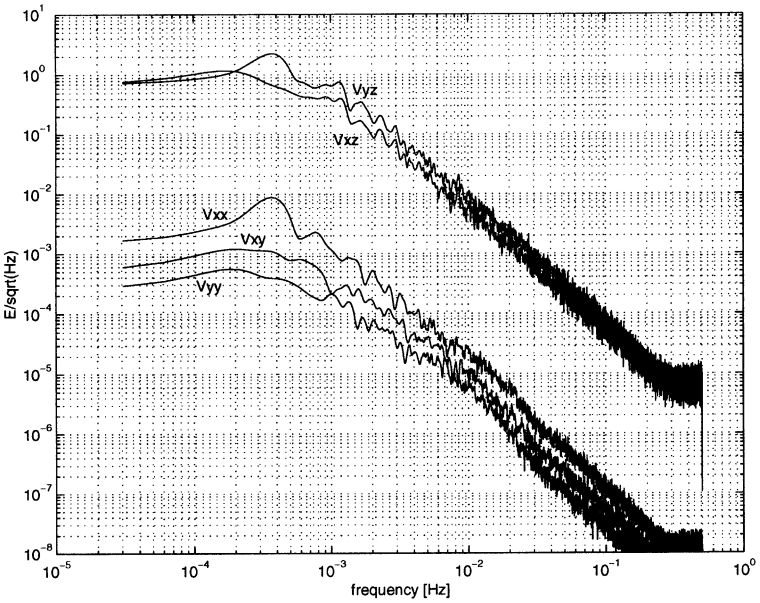

Fig. 7. Satellite pointing error.

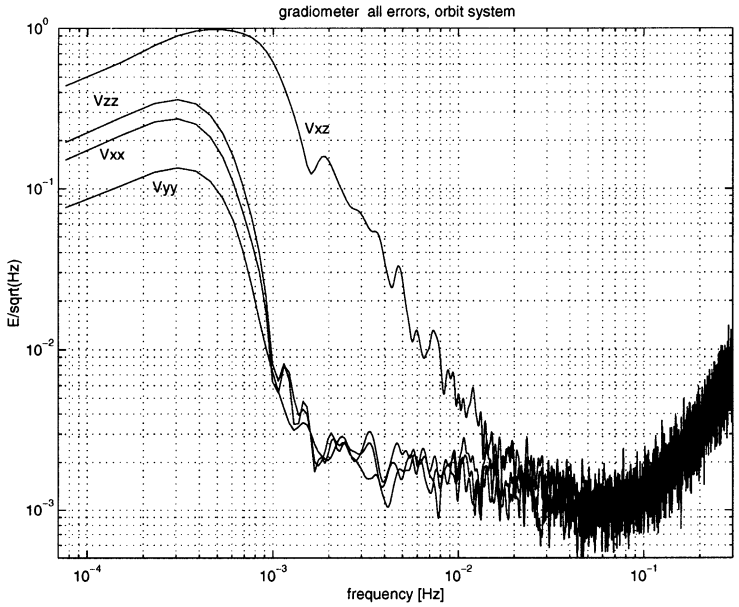

Fig. 8. Result of the gradiometer error simulation, where all error effects have been switched on.

diagonal gravity gradients. The simulation shows that the mission requirement in the measurement bandwidth from 0.005 to 1 Hz is fulfilled for the diagonal components. Moreover, the V_{xz}- and V_{zx}-components support the gravity field determination at the very high frequencies and help to derive potential coefficients up to degree and order 300 with significant accuracy. By propagating these error results to the end-products, it can be shown, that GOCE will achieve the scientific goals, which are 1 cm (geoid error) resp. 1 mGal (gravity anomaly error) at half wavelength down to 100 km. The GOCE gravity field will be used for further applications in oceanography (determination of the sea surface topography from the combination with altimetry), solid Earth physics (the spatial variations of the gravity field represent one of the few observables of the Earth's interior) and geodesy (e.g. for the unification of global height systems or levelling with GPS).

The effects of further error sources like time-dependent scale factors and misalignments or possible non-linear couplings have still to be investigated. Preliminary investigations (not shown in this paper) indicate, that the mission requirements in the MBW will also be kept under these more realistic conditions.

Acknowledgements

This work has been funded in part under the ESA/ESTEC contract No. 12735/98/NK/GD. We are mostly indebted to our colleagues from the SID-Consortium, existing of SRON (Space Research Organisation Netherlands), IAPG (Institut für Astronomische und Physikalische Geodäsie) and DEOS (Delft institute for Earth-Oriented Space research). The help of Alenia Aerospazio, Italy, is also greatly acknowledged.

References

Willemenot, E., Touboul, P., 1998. Capacitive Gradiometer Modelization—First Simple Model. Published document from ONERA.

Willemenot, E., 1998. GOCE Phase A-PM1. Unpublished document from ONERA.